

Adaptive Kinetic-Fluid Solvers for Heterogeneous Computing Architectures

Sergey Zabelok^a, Robert Arslanbekov^b, Vladimir Kolobov^b

^a*Dorodnicyn Computing Center of Russian Academy of Sciences, Vavilova-40, Moscow, 119333, Russia*

^b*CFD Research Corporation, Huntsville, AL 35805, USA*

Abstract. This paper describes recent progress towards porting a Unified Flow Solver (UFS) to heterogeneous parallel computing. UFS is an adaptive kinetic-fluid simulation tool, which combines Adaptive Mesh Refinement (AMR) with automatic cell-by-cell selection of kinetic or fluid solvers based on continuum breakdown criteria. The main challenge of porting UFS to graphics processing units (GPUs) comes from the dynamically adapted mesh, which causes irregular data access. We describe the implementation of CUDA kernels for three modules in UFS: the direct Boltzmann solver using discrete velocity method (DVM), the Direct Simulation Monte Carlo (DSMC) module, and the Lattice Boltzmann Method (LBM) solver, all using octree Cartesian mesh with AMR. Double digit speedups on single GPU and good scaling for multi-GPU have been demonstrated.

Keywords: Unified Flow Solver, Adaptive Mesh Refinement, Discrete Velocity Method, Boltzmann Kinetic Equation, Direct Simulation Monte Carlo, Lattice Boltzmann Method, Graphics Processing Units, CUDA, MPI.

PACS: 05.10.-a 51.10.+y 52.25.Dg 52.30.-q

INTRODUCTION

It is well known that transport phenomena can be described by either atomistic (kinetic) or continuum (fluid) models. Kinetic description in terms of particle distribution functions is more detailed and computationally more expensive compared to the continuum description in terms of density, mean velocity and temperature. For this reason, adaptive kinetic-fluid models are being developed, which enable selecting appropriate kinetic and fluid solvers for different system components to achieve maximum fidelity and efficiency.^{1, 2, 3}

Two methodologies have been used to solve the kinetic equations: statistical particle-based methods such as Direct Simulation Monte Carlo (DSMC) or Particle-in-Cell (PIC)^{4, 5} and direct numerical solutions using computational grid in phase space.^{6, 7} Fluid models are based on the first few moments of the kinetic equation expressing conservation laws for the particle density, momentum, and mean energy. Mesoscopic models such as Lattice Boltzmann Method (LBM) use a minimal set of discrete velocities to simulate dynamics close to equilibrium. Adaptive kinetic-fluid models apply different solvers in selected regions of physical or phase space for efficient description of multi-scale phenomena in complex systems. Appropriate solvers are selected using sensors locally detecting phase space regions where a kinetic approach is required and where more simple fluid models can be applied.

For gas dynamics in mixed rarefied-continuum regimes, the adaptive kinetic-fluid approach has been first realized using an Adaptive Mesh *and* Algorithm Refinement (AMAR) methodology introduced for DSMC-fluid coupling.⁸ Later, a Unified Flow Solver (UFS) has been developed to combine Adaptive Mesh Refinement (AMR) with automatic cell-by-cell selection of either direct Boltzmann solver or Euler-Navier-Stokes solvers⁹ based on continuum breakdown criteria.¹ Recently, the AMAR methodology has been extended for hybrid modeling of radiation transport¹⁰ and is now being developed for plasma simulations.²

Figure 1 shows the basic architecture of the AMAR framework, which was implemented on top of Gerris - an open source computing environment for solving partial differential equations with AMR.¹¹ The original physical model of the Gerris Flow Solver (GFS) includes time-dependent incompressible variable-density Euler, Stokes or Navier-Stokes equations for two-fluid flow with VOF method. GFS provides with entirely automatic mesh generation for complex geometries and portable parallel support using the MPI library, dynamic load-balancing, parallel offline visualization and VOF advection scheme for interfacial flows. GFS uses a coarse-grained parallelization based on “Forest of Trees” (FOT) approach.¹²

AMAR enables the higher degree of adaptation by using different physical models in different parts of the computational domain. The computational domain is decomposed into kinetic and fluid cells using physics-based continuum breakdown criteria. This methodology was first implemented for mixed rarefied-continuum flows and later extended for hybrid model of radiation transport coupling a Photon Monte Carlo (PMC) solver with a diffusion model of radiation transport, with the solver selected based on the local photon mean free path.¹⁰

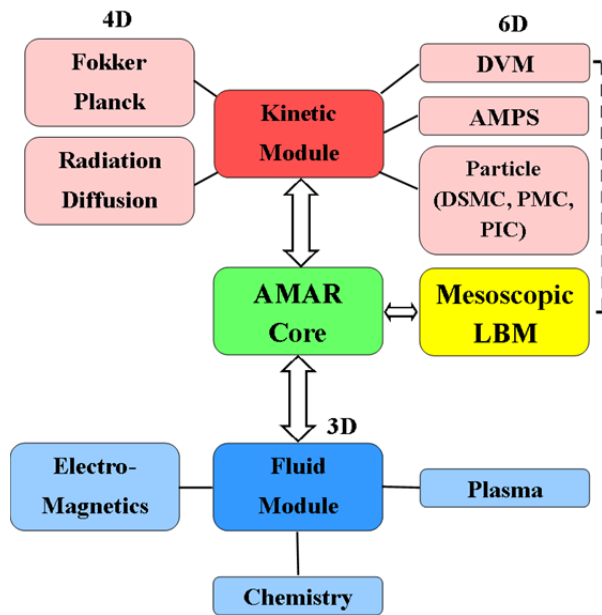


Figure 1: The AMAR framework

The Kinetic Module in the AMAR framework can solve Boltzmann, Vlasov, and Fokker-Planck kinetic equations using different methods. Eulerian kinetic solvers use the Discrete Velocity Method (DVM) for solving kinetic equations. The recently developed Adaptive Mesh in Phase Space (AMPS) methodology¹³ can adapt mesh in both physical and velocity spaces. The DSMC and PMC are based on Lagrangian transport models.¹⁴ A mesoscopic LBM solver uses a minimal set of discrete velocities adapted from the DVM kinetic solvers.¹⁵

This paper describes our efforts towards adapting the AMAR framework for heterogeneous computing. Modern high performance computing makes use of Single

Instruction Multiple Data (SIMD) vector processors. Graphical Processing Units (GPUs) were pioneers in this kind of computing, especially after NVIDIA introduced CUDA. Intel has introduced a similar architecture with the Phi coprocessor based on the Intel Many Integrated Core (MIC) Architecture. GPUs have become powerful data-parallel computation accelerators

for a wide range of devices from high-end supercomputers to battery-powered mobile devices, tablets, and laptops.¹⁶ For programs that map well to GPU hardware, GPUs offer a substantial advantage over multicore CPUs in terms of performance, performance per dollar, and performance per transistor and energy efficiency.

Porting existing computational algorithms and software for heterogeneous CPU-GPU architectures involves some effort. The “low-hanging fruit,” so-called *regular* codes require no significant change in program structure or algorithm when being ported to GPUs.¹⁷ Irregular codes associated with dynamic data structures (such as graphs, trees, etc.) are more difficult to port. Nevertheless, it has been demonstrated that GPUs are capable of accelerating many irregular codes, and there is plenty of exploitable parallelism available even in irregular codes.¹⁸

Kinetic solvers are best suited for parallel computing. Impressive acceleration and excellent multi-GPU scaling have been demonstrated by several groups using particle^{19,20} and mesh-based methods with structured meshes.^{21,22} We have recently demonstrated double digit speedups on a single GPU²³ and good scaling for multi-GPU for the direct Boltzmann solver using the discrete velocity method (DVM), the DSMC module, and the LBM solver, all using (semi-structured) octree Cartesian meshes with AMR.¹⁵ Coupled Vlasov and two-fluid codes have recently been demonstrated using GPU for Vlasov solvers in locally selected kinetic domains.³

This paper describes first results of porting adaptive kinetic-fluid solvers to heterogeneous CPU-GPU systems. The tree-based adaptive Cartesian mesh of UFS poses specific challenges for porting to heterogeneous multi-GPU systems due to irregular data access. Furthermore, different cost of kinetic and fluid cells should be taken into account when developing parallelization algorithms. We first describe details of parallel implementation of the AMAR technology and illustrate hybrid simulations of supersonic flows using GPUs for the kinetic cells only. Then, we describe details of the implementation of CUDA kernels for three modules in UFS: the DVM Boltzmann solver, the DSMC module, and the LBM module.

PARALLEL IMPLEMENTATION OF AMAR

There are two parallel implementations of UFS solvers. The fine grained parallelization using Space Filling Curves (SFC) was first described in Ref. [24]. The coarse grained parallelization using Forest of Trees (FoT) is described in Ref. [12].

Fine Grained Parallelization using Space Filling Curves

The computational grid in GFS is generated by subsequent division of square boxes into smaller boxes with linear dimensions equal to half of the initial dimension (left part of Figure 2). The procedure of creating the computational mesh can be represented by a tree (the right part of Figure 2). The root of the tree (0th level) corresponds to initial cube, the first level corresponds to 4 (in 2D) or 8 (in 3D) cubes obtained by division of the initial cube, etc. The computational cells correspond to leaves of the tree. All computation procedures are called only for the leaves of the tree. To perform computations for a part of the domain (for instance, the sub-domain shown by blue color in Figure 2), one introduces a flag for each leaf to identify whether or not the cell belongs to the selected sub-domain. If a cell is a parent cell for a set of cells, it is flagged only if at least one child cell belongs to the selected sub-domain. After introducing flags, the procedure

of cell traversing is modified to visit only the cells belonging to selected sub-domain. As shown on the right part of Figure 2, only the branches connected by solid lines are traversed. To specify boundary conditions, additional cells (hatched in Figure 2) are used. The branches corresponding to the boundary cells are shown by dashed lines on the graph. The boundary cells are marked using a different flag, and can be traversed separately by the code.

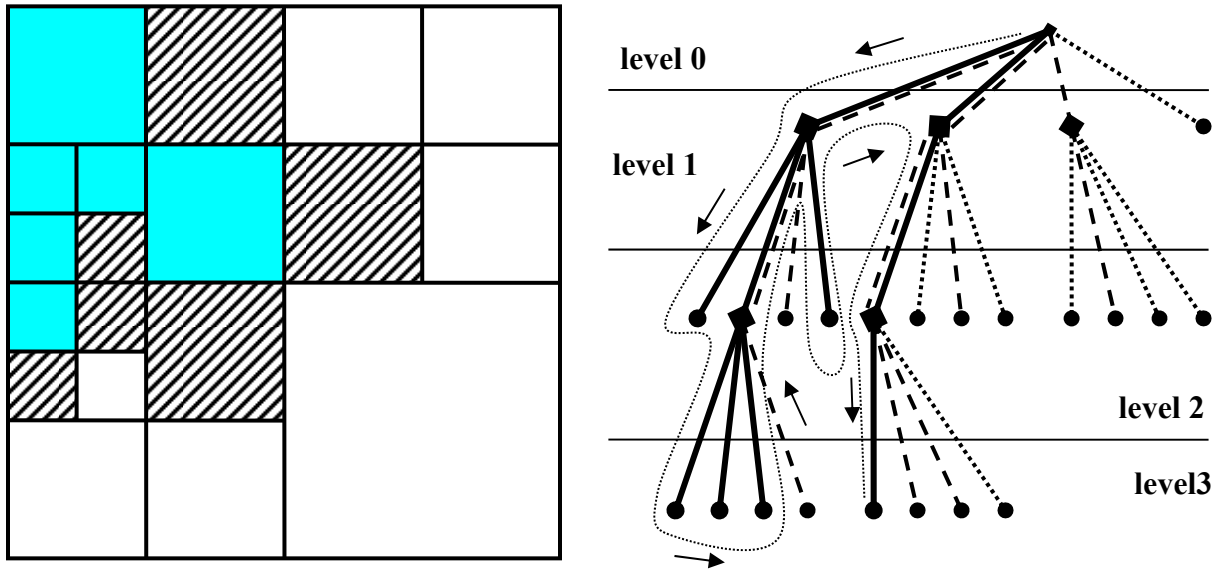


Figure 2: The computational mesh and the tree corresponding to it.

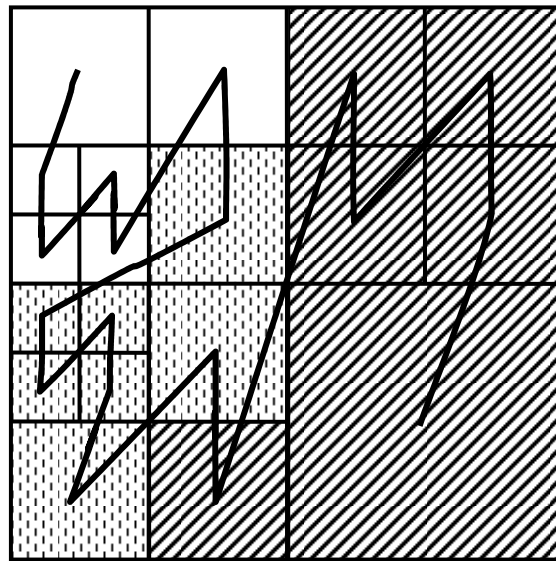


Figure 3: Domain partitioning obtained with SFC algorithm for the case of 3 processors.

Dynamic domain decomposition was performed using space filling curves (SFC) as illustrated in Figure 3. During sequential traversing of the cells by natural order, the physical space is filled with curves in N-order (Morton ordering). After this ordering of the cells, a weight is assigned to each cell based on the CPU time required to perform computations in this cell. Kinetic cells have

a much larger weight compared to the continuum cells. Furthermore, the array modified with corresponding weights, is subdivided into sub-arrays equal to the number of processors, in such a way that the weights of each sub-arrays are approximately the same. This method allows very efficient domain decomposition between different processors.

Coarse Grained Parallelization using Forest of Trees

The FOT algorithm consists of dividing the computational domain into boxes with a Cartesian tree built in each box. This represents a coarse-grain parallelization algorithm since the CPU load balancing can be done only in terms of the building (root) boxes. Each CPU operates on a given number of boxes, and the computational grid is stored only on the CPU it belongs to. During grid adaptation these boxes are exchanged between the CPUs for dynamic load balancing (DLB). Each box has its own ID number and a set of boxes on each host CPU share the same PID (Processor ID) number.

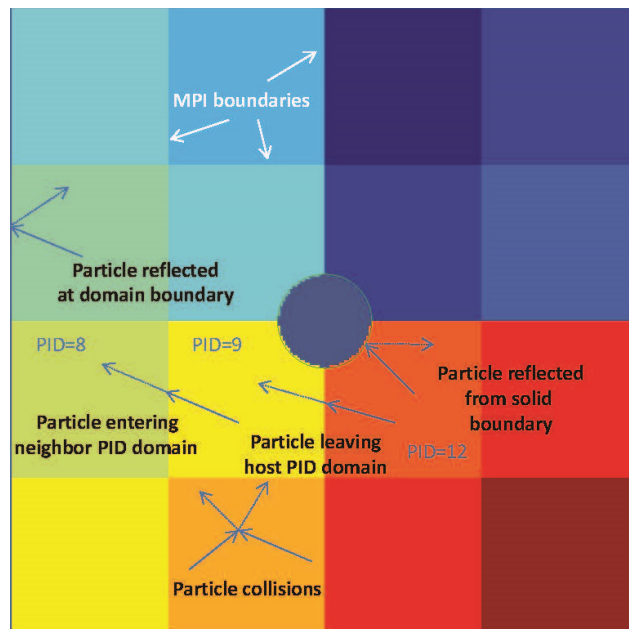


Figure 4. Processor ID partitioning for 16 CPU/GPUs for the problem of heat transfer. Also shown are illustrations of particle interactions with solid surface/phases, with other particles and with domain and MPI boundaries.

Figure 4 shows an example of initial domain decomposition into 16 boxes for DSMS simulation of a heat transport between a cold solid cylinder immersed into a square box with hot walls. At the beginning of simulations, particles are initialized in each PID domain. These particles start to move and interact with each other, with domain boundaries, and with solid surfaces/phases immersed into the domain, as illustrated in Figure 4. Particles (their position, velocity, remaining move time, etc.) which hit an MPI boundary are stored in a special list and then removed all together from their PID domain. Knowing the direction of the box boundary face a particle hits, its neighbor PID (e.g., PID=8 in Figure 4) is determined. This neighbor PID is then used for the thus stored particles to send to and to receive from (PID=12 in Figure 4). The neighboring PIDs receive and then add these particles for further processing during the next time step. Then this procedure repeats for the next time step and so on.

Example of hybrid parallel CPU-GPU simulations of a complex gas flow

Figure 5 shows an example of hybrid, kinetic-fluid simulations of supersonic flow over a X-51A waverider scramjet at $M=5$ and $Kn=0.01$ (per vehicle length) obtained on a CPU-GPU NASA cluster with 58 GPUs. The total number of adapted computational cells is 3.5M, and the total number of kinetic cells (shown by brown color in Figure 5, right) is $\sim 1.2M$. The kinetic cells were activated in the regions of large local Knudsen number combined with large flow gradients (see Ref. [1] for details of computing the continuum-kinetic switch). Fine-grained domain decomposition is obtained using SFC; GPUs are used only in the kinetic cells to speed up the Boltzmann solver's advection and collision modules. Double digit speedup for the kinetic cells and good DLB (thanks to the fine-grained SFC algorithm) between the nodes were obtained (see below for details).

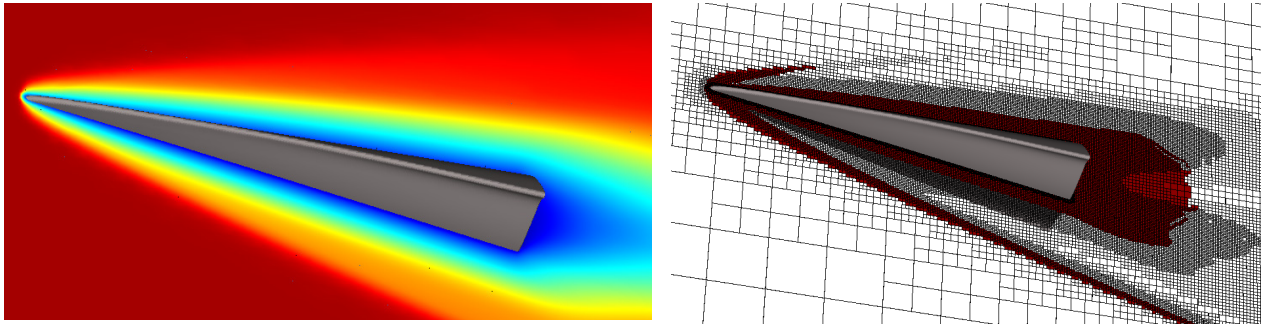


Figure 5: Mach number (left), computational mesh and kinetic domain (brown cells, right) around a Waverider scramjet.

The details of the CUDA implementation of different UFS solves for GPU computing are described below.

BOLTZMANN SOLVER

The UFS-Boltzmann solver is based on the direct numerical solution of the Boltzmann kinetic equation using DVM, which has the following form in non-dimensional variables:

$$\frac{\partial f}{\partial t} + (\vec{\xi}, \vec{\nabla}_x f) = \frac{1}{Kn} I(f, f).$$

Here f is the 7-dimensional distribution function depending on scalar time t , and on two 3-dimensional vectors (coordinate \vec{x} and molecular velocity $\vec{\xi}$) and I is the 5-fold collision integral with quadratic dependence on distribution function. The Knudsen number Kn is the ratio of the mean free path to the characteristic spatial scale, which is a measure of the gas rarefaction degree.

The numerical solution of the Boltzmann equation is based on discrete velocity approach, in which approximation of the distribution function on regular rectangular mesh in velocity space and adaptive non-uniform Cartesian mesh in physical space is considered. The left-hand side of the Boltzmann equation (advection operator) is evaluated with finite volume (FV) technique, the

right-hand side (collision integral) is computed using the stochastic method with Korobov nodes (see details in Ref [1]).

This numerical scheme has been successfully ported to GPU and demonstrated good speedup on single GPUs.²⁵ We have developed CUDA kernels for the advection and collision operators. It should be mentioned that UFS uses fast method for collision integral computations, in which the computational times for collision and advection parts in many problems are of the same order, and that is why it is necessary to construct an advection kernel for GPU, in addition to the collisional kernel. In many other methods, implemented on GPU^{26,27}, the time for collision integral computations was much larger than the advection, so it was not necessary to construct an effective advection scheme.

The method for numerical solution of the Boltzmann equation with CUDA GPU is based on specific presentation of the required data. In it the distribution function points are reordered in such a way that they form vectors for which the same arithmetical operations are performed. This type of vector data presentation allows effective use of CUDA GPU capabilities.

Advection Algorithm

The algorithm for approximation the advection operator on GPU is based on the properties of FV advection scheme used in UFS for approximating convective part of the Boltzmann equation. This numerical scheme can be written as follows:

$$\begin{aligned} \frac{f_{i,j}^{n+1} - f_{i,j}^n}{\Delta t} + \xi_{x,i} \sum_{k=1,\dots,m_x(i,j)} a_x(k,i,j) f_{i,\alpha_x(k,i,j)}^n + \xi_{y,i} \sum_{k=1,\dots,m_y(i,j)} a_y(k,i,j) f_{i,\alpha_y(k,i,j)}^n \\ + \xi_{z,i} \sum_{k=1,\dots,m_z(i,j)} a_z(k,i,j) f_{i,\alpha_z(k,i,j)}^n = 0. \end{aligned}$$

Here n corresponds to the time step, i and j enumerate the points of discrete mesh in velocity and physical space respectively. In the case of a Cartesian mesh the coefficients in the above formula (at a given point of physical space) are the same for molecular velocities belonging the same octant (the components of molecular velocities have the same signs), i.e. for the numbers $m_\beta(i,j)$, coefficients $a_\beta(k,i,j)$ and indexes $\alpha_\beta(k,i,j)$ $\beta=x, y, z$ the dependence on the index i can be replaced with the dependence on $\text{sign}(\xi_{\beta,i})$. This is used in algorithm for numerical advection scheme.

The algorithm for CUDA computations consists of the following steps:

1. Create 8 **groups** of velocity points with the same signs of velocity components. The first group corresponds to signs (-, -, -), the second one – to (-, -, +), etc. Rearrange the points of velocity space in such a way that for a given point each **group** to be located in one consecutive block of memory.
2. Create an array for the distribution function storage.
3. Store the distribution function for different points of physical space in a single array, with the points in velocity space to be ordered in the same way as it is done in step 1.

4. For each point in physical space j store numerical scheme for each **group** of velocity points, i.e. record the quantity of stencil points $m_\beta(\text{sign}(\xi_{\beta,i}), j)$, stencil point numbers $\alpha_\beta(k, \text{sign}(\xi_{\beta,i}), j)$, the stencil weights $a_\beta(k, \text{sign}(\xi_{\beta,i}), j)$.
5. Copy all the data obtained in steps 2 and 4 to device memory.
6. Execute the advection kernel.
7. Copy results from device to host memory.

Step 1 is done once before the 1-st time step. Steps 2 and 4 are redone each time the spatial mesh is changed. Other steps are executed every time step.

The advection kernel (step 6) takes the addresses of arrays of the distribution function and stencil parameters as parameters. A single thread block computes the advection contribution of all velocity points of one **group** of velocity points for one point of physical mesh, with each thread corresponding to a point of velocity space. The stencil parameters are copied to shared memory. The molecular velocity components, which are different for each thread, are computed once per kernel execution and are stored in the register memory. Thus the procedure of computing the advection operator consists of a sequence of vector multiplication (the distribution function for points of one velocity **group**) by a number from shared or register memory operations, which is a very effective operation for SIMD devices. For CUDA GPUs this procedure also allows to avoid problems with coalescing.

Collision Integral

The collision integral for the Boltzmann equation is approximated by the following formula:

$$I_{i,j}^{*n} = -f_{i,j}^n \sum_{k=1, \dots, M(i)} b(k, i) f_{\gamma(k,i),j}^n + \sum_{k=1, \dots, M(i)} c(k, i) f_{l(k,i),j}^n f_{m(k,i),j}^n.$$

The number of trials $M(i)$, the indexes $\gamma(k, i)$, $l(k, i)$, $m(k, i)$ and the coefficients $b(k, i)$, $c(k, i)$ are the same for all points of velocity space. The star superscript denotes that this formula gives an intermediate approximation of the collision integral, which does not satisfy the conservation laws. In order to satisfy the mass, momentum and energy conservation, the computations of the collision integral are divided into 3 steps:

1. Computations of the collision frequency

$$B_{i,j}^n = \sum_{k=1, \dots, M(i)} b(k, i) f_{\gamma(k,i),j}^n$$

2. Computations of the inverse collisions integral

$$C_{i,j}^n = \sum_{k=1, \dots, M(i)} c(k, i) f_{l(k,i),j}^n f_{m(k,i),j}^n.$$

3. Conservative correction

$$I_{i,j}^n = -f_{i,j}^n P_{i,j}^n C_{i,j}^n + B_{i,j}^n,$$

$$P_{i,j}^n = \left(1 + d_0(j) + d_x(j)\xi_x(j) + d_y(j)\xi_y(j) + d_z(j)\xi_z(j) + d_2(j)\vec{\xi}^2(j) \right).$$

The five coefficients $d_\beta(j)$ of the polynomial $P_{i,j}^n$ for each spatial point j in the last operation (conservative correction) are found from the system of five linear equations, which are numerically equivalent to the conservation laws.

The algorithm for CUDA computations consists in the following steps:

1. Create an array for the distribution function storage.
2. Store the distribution function as an array of vectors with each vector corresponding to a single point of velocity space and to all points of physical space.
3. Compute the number of trials $M(i)$, the indexes $\gamma(k, i)$, $l(k, i)$, $m(k, i)$ and the coefficients $b(k, i)$, $c(k, i)$ and store them in a corresponding array.
4. Copy arrays from steps 2 and 3 to device memory.
5. Create arrays for device storage of collision frequency and inverse collision integral.
6. Execute kernel for computations of collision frequency and inverse collisions integral.
7. Reorder the distribution function, collision frequency and inverse collision integral in device memory, for them to become the arrays of vectors with each vector corresponding to a single point of physical space and to all points of velocity space. This is done by a simple kernel which perform transpose operation.
8. Execute conservative correction kernel.
9. Copy the results to host memory.

In the collision kernel (step 6) a single thread block computes the collision frequency and inverse collisions integral for the entire physical mesh for one point of velocity space, with each thread corresponding to a cell in physical space. The parameters $M(i)$, $\gamma(k, i)$, $l(k, i)$, $m(k, i)$, $b(k, i)$, $c(k, i)$ are the same for all threads inside the thread block, and thus they are copied to the shared memory. Thus procedure for computing collision frequency and inverse collisions integral consists of sequence of multiply vector (the distribution function for all points of physical mesh for a given velocity point) by a number from shared memory operations, which is (the same as for advection operator) very effective operation for SIMD devices, and also allows to avoid problems with coalescing for CUDA GPUs.

In the conservative correction kernel a thread block corresponds to a cell in physical space. At first the matrix elements and the right-hand side vector of the 5x5 linear system are computed inside each block. These elements are obtained as moments of the distribution function. Every thread inside the block computes the contribution to a moment of one velocity point, and after that the sum of all contributions is gathered to the thread with number 0 with a $O(\log_2[\text{number_of_threads}])$ operations. The next step is to solve the 5x5 linear system which is easily done with the Gauss method using 1-st 25 threads of block. The last operation in the kernel is to obtain the value of collision integral. For this the vector of polynomial $P_{i,j}^n$ values is constructed (only shared and register memory is used for polynomial computations). After that the component multiplication and addition of vectors $P_{i,j}^n$, $f_{i,j}^n$, $B_{i,j}^n$ and $C_{i,j}^n$ is done.

Computational tests demonstrated speedup of advection kernel itself was from 15 to 40 times for different CPU and GPU combinations. The calculations of the collision integral in UFS-Boltzmann-GPU have demonstrated speedups of up to ~ 50 .¹⁵

Multi-GPU Implementation of the Boltzmann Solver

A multi-GPU algorithm was implemented for UFS-Boltzmann solver for the particular hardware architecture with one GPU attached to one CPU. The SFC method of UFS was used to uniformly partition the computational domain (in physical space) between processors. Partitioning in physical space allowed leaving the collision integral computations unchanged, because the collision integral is calculated locally.

The advection algorithm includes the following items. The memory storage for the distribution function is arranged in such a way that the distribution function of the cells from the considered CPU (inner cells) are stored before the cells, which are included in a stencil for this CPU but belong to other CPU (ghost cells). The distribution function for ghost cells is gathered from other CPUs using MPI procedures. The device memory is arranged in the same manner as the host memory, the distribution function is copied from host to device using `cudaMemcpy()` function. The advection kernel, which was previously developed for a single GPU code, is called to process only the part of device memory corresponding to inner cells (but this kernel utilizes the ghost cells distribution function). The latest step of the algorithm is to gather the advection contribution from device to host. The scheme for this algorithm is presented in Figure 6.

The described algorithm was implemented and tested on a 2-core computer with 2 GPUs. The speedup compared to a single CPU-GPU runs was 1.8 for a 3D problem of rarefied subsonic flow over a sphere.

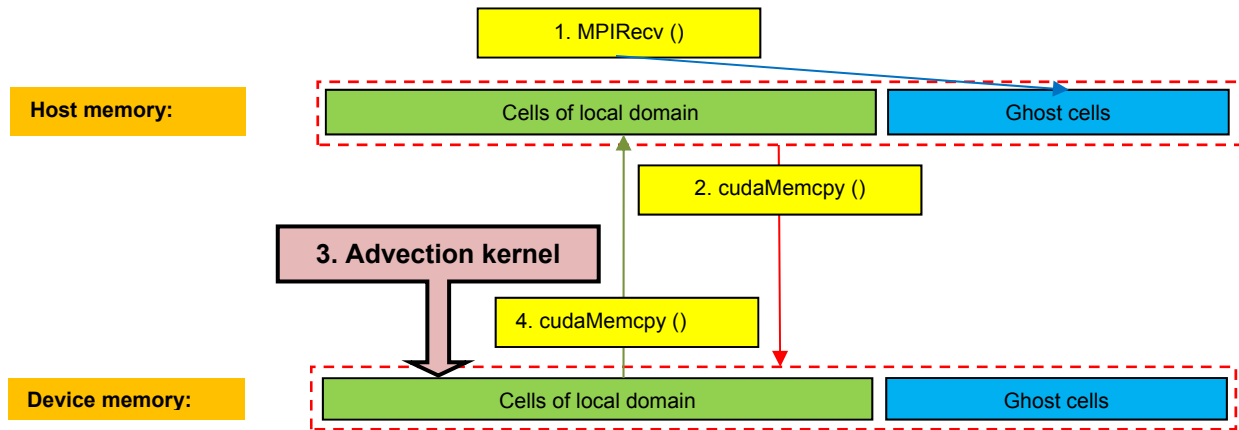


Figure 6: Schematic algorithm for MPI-CUDA implementation of the advection part of the UFS-Boltzmann solver.

DIRECT SIMULATION MONTE CARLO

The DSMC module in UFS utilizes single mesh for particle transport, inter-particle collisions, statistics collection and visualization.¹⁴ The AMR capabilities based on local flow properties (the particle mean free path, gradients of gas flow parameters, embedded surface curvature, etc.)

can efficiently perform the same functions as transient subcells or other collision partner selection options available in modern DSMC codes. The tree-based data structure of UFS-DSMC allows straightforward and efficient dynamic grid refinement and coarsening and removes the necessity of using subcells and additional models of collisional partners' selection.

The particle data storage in UFS-DSMC is cell-based, which means that each cell has a list of particles assigned to it. This allows efficient selection of collisional partners during collision step. During the free flight, when a particle crosses a face of a cell, it is removed from the list of its old cell and added to the list of a neighboring cell. The particles move inside each computational cell until they hit a cell face or a wall/boundary face. Particle tracing is efficient since all full cells are square or cubic; in cut cells, an additional solid face is checked for possible reflection and appropriate boundary conditions are applied when this face is crossed. Since a cell neighbor of a face which has been hit by a particle can be at a higher level, a new particle cell location is assigned depending on which part of the face has been traversed. During refinement of a coarse cell, particles are stored in new cells according to their position in this coarse cell. During cell coarsening, particles in fine cells are assigned to a new coarse cell. No special treatment (such as assigning different weights) is carried out to account for different volumes of cells on the adapted grid. Moreover, no special treatment of small cut cells is performed. The latter can lead to significant statistical scatter of the surface data (such as skin friction and heat flux). To tackle this issue, we have implemented special routines which traverse all cut cells at a given coarse level (usually corresponding to initial uniform grid). Inside each such (non-leaf) cell, all leaf cut cells are visited and the surface data are weight averaged with the corresponding cut-face surface area. This procedure allows significant reduction of statistical scatter in the calculated surface fluxes and provides similar advantages to a decoupling of surface elements from the grid structure as is usually done in other DSMC codes.

DSMC simulations of rarefied flows over moving objects

The UFS solvers deal with boundary cells using two techniques: 1) cut-cell technique combined with cell merging¹¹ and 2) Immersed Boundary Method (IBM).²⁸ UFS-DSMC uses the cut-cell technique. For moving-body capabilities, we utilize the corresponding module in the GFS framework which is based on the use of the GTS library²⁹ to represent static or moving immersed solid objects. When a GTS-represented body is moved, vertices of each surface mesh triangle are displaced by a small amount $\Delta\vec{r} = \vec{V}_{body}\Delta t$, where \vec{V}_{body} is the surface velocity and Δt the integration time step. The old surface grid at a previous time step $t - \Delta t$ and the new surface grid at current time step t are then stored, and the new volume grid is re-cut (to achieve second order accuracy in time, a surface grid from a time step $t - 2\Delta t$ is also stored). During this grid re-cutting step, the new volume grid undergoes the procedure called "hole cutting," in which one of the following 3 situations are realized: 1) position of a solid panel changes in cut cells, 2) new cut or full cells are created and 3) some cells become fully embedded into the solid and are thus destroyed. In the UFS-DSMC Module, particles (which are characterized by position, velocity, internal energy, etc.) are stored in each grid cell including the cut cells; such data storage allows straightforward implementation of the moving-body capabilities. Namely, when a solid panel moves in a cut cell, those particles which find themselves inside the solid are considered as having collided with the wall during the solid panel displacement and thus having acquired the wall velocity \vec{V}_{body} ; the new particle position is then assumed to be close to the new wall position

with the wall panel being slightly displaced away from it. When a new cell is created, it is assumed that no particles are initially present there. Once a new solid body position is set, particles are allowed to freely move and collide with other particles and with the (new and old) solid panels. When a particle collides with a solid panel (with a given temperature T_{body}), it is set to acquire the local translation velocity of the solid panel \vec{V}_{body} (and its temperature T_{body}). During the next time step, the procedure repeats and so on.

We first demonstrate the UFS-DSMC results for rarefied flows over moving bodies. Figure 7 shows examples of simulations for Ar gas at rest with a density of $8.5 \times 10^{19} \text{ m}^{-3}$ and temperature of 200 K perturbed by a star-shaped body moving with a rotational speed of 2,000 rad/s and translational speed of 1,000 m/s. The right part shows two ellipsoids moving with a rotational speed of 2,000 and 1,500 rad/s, correspondingly, and the same translational speed of 1,000 m/s. The grid adapts to the boundary layer around the bodies and to the flow gradients. One can see in Figure 7a and Figure 7b that the adapted grid allows properly resolving flow features with reduced computing cost by adding computational cells in the regions where it is necessary and coarsening the grid in the regions with small flow gradients to reduce the particle count. We have found that at least 10M particles are required to run this transient case to achieve acceptable statistics.

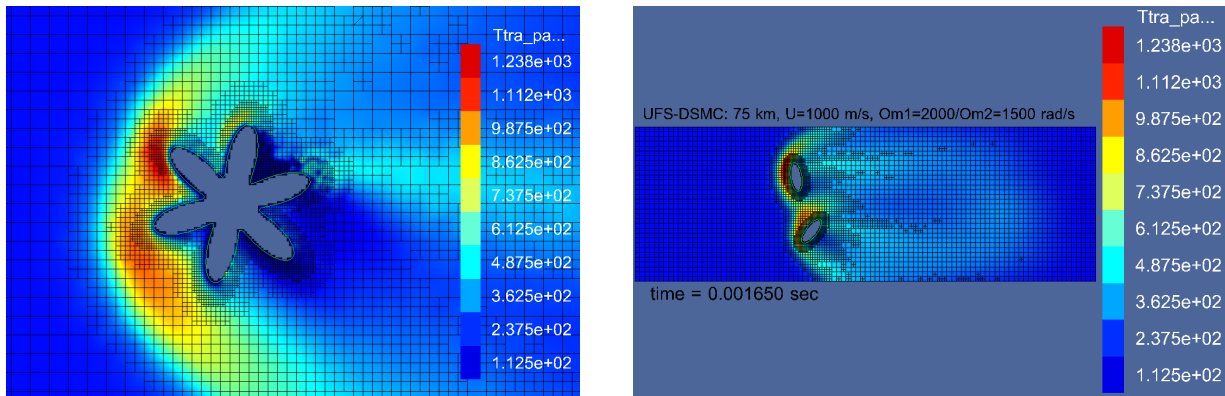


Figure 7: Adapted computational grid colored by translational temperature for moving star-shaped body (left) and two ellipsoids in relative motion (right) with 10M particles.

Parallel capabilities in UFS-DSMC were implemented using MPI protocols. We have observed a close to ideal scaling with increasing number of processors.

Single-GPU Implementation of the DSMC Solver

A single-GPU implementation of UFS-DSMC was first reported in Ref. [25]. An all-device (i.e., GPU) computational approach³⁰ is adopted where the entire computation is performed on the GPU device, including particle moving, indexing, particle collisions and state sampling. Communication between the GPU and host (CPU) is only performed to enable multiple-GPU computation.

Each part of UFS-DSMC-GPU was realized via a corresponding GPU kernel. Execution of a code on GPU requires that all data available on CPU host be prepared in a way that the GPU

device can handle it. So, special data structures are required to be implemented. These data contain such information as simulation parameters, grid, cell, faces, neighbors, types of cells, faces, etc. On a host CPU, such information can be accessed via pointers and on GPU, it has to be accessed via indices.

CUDA Kernels for Particle Movement, Collision and Sampling

Using the prepared cell and face data fields, particle movement is executed. Each particle is followed by a separate thread until the particle hits a face of a cell in which it is currently located. At cells faces, particles are reflected (solid faces or symmetry/diffusion reflection boundaries) and they are moved to its neighbor using neighbor indices (on coarse-fine interfaces, the new particle cell is decided depending on the location where the particle hits the face). The particle movement is carried out for old particles (already present in the domain) as well as for new particles generated at inflow/inlet boundaries.

When collisions are activated, collisions in each cell are treated by a separate thread. Particles are indexed and collision pairs are selected in each cell; new particle velocities are calculated based on the conservation laws. During particle movement and collisions, sampling of particle locations and velocities needs to be performed. For steady-state simulations, this is usually done starting from some start up step during a simulation. The particle sampling kernels are implemented using cell based kernels (each cell is treated by a separate thread). Shared memory is used to efficiently calculate the required sums of particle quantities over all particles in each cell.

Multi-GPU Implementation of the DSMC Solver

For hybrid MPI-CUDA parallelization paradigm, domain decomposition was performed using the FOT method. In this method, the MPI protocol is used to exchange data from memory of all MPI processors and synchronize. CUDA is used to put the DSMC-related simulation components on GPU, and for data transfer between CPU (host) memory and GPU (device) global memory. For data exchanges between global memory of different GPU devices (for example, from device-A to device-B) we use the CUDA API function `cudaMemcpy()` to transfer data from device-A to host-A. Next, the data is transferred from host-A to host-B using the MPI protocols. Finally, we use `cudaMemcpy()` to transfer data from host-B to device-B. This flexible method allows a single subroutine to manage communications without concern for (i) the device type, or (ii) if the device is located on the same physical node (see Ref.[30] for more details).

The implementation of MPI-CUDA capabilities for DSMC followed several steps:

- A GPU kernel to calculate positions of all particles over a time step dt .
- Each particle's deterministic motion is handled by a CUDA thread, using data held entirely in global memory.
- Particles determined to have left the current GPU's simulation domain are placed into a buffer (in the device, and finally on the host) in preparation for migration to other GPU devices.
- Introduce new particles based on inlet boundary conditions.

- Send and receive from buffers of all MPI processors (host) with the MPI API protocols `MPI_Send()` and `MPI_Recv()`.
- Reallocate particles from buffers into their newly allocated GPU's global memory.

Multi-GPU scaling was studied on the NASA Pleiades cluster with 64 Westmere nodes with one NVIDIA Tesla M2090 GPU per node. Each GPU with high speed memory is connected to the Westmere node via a PCI Express bus, and the nodes are connected via high-speed Infiniband. Figure 8 shows the real computational times (per 2,500 time steps) as a function of the number of GPUs. One can see that a very good scaling is obtained with the power law scaling factor being 0.8 (factor of 1 means ideal scaling). This proves a good efficiency of the hybrid MPI-CUDA algorithm for DSMC.

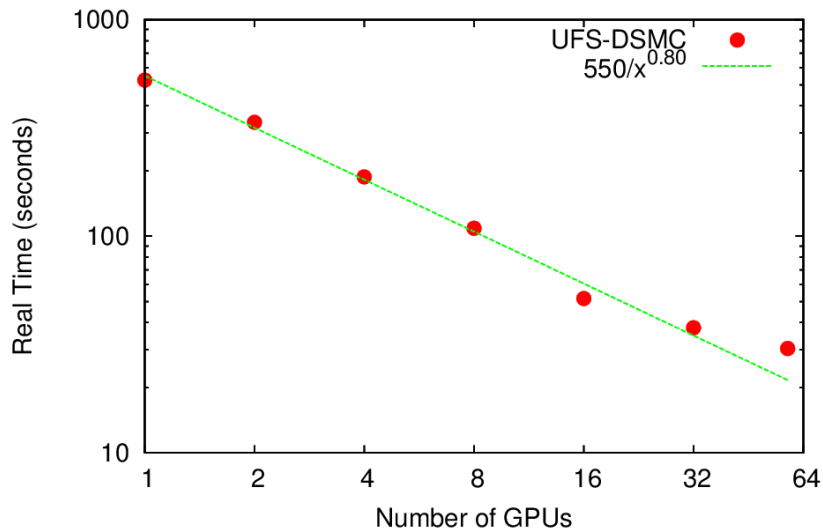


Figure 8: Computing time (per 2500 time steps) as function of number of GPUs for a problem of heat transfer with 30M particles.

LATTICE BOLTZMANN METHOD

The LBM Module in UFS is a subset of the DVM kinetic solvers. The DVM kinetic solvers allow using velocity grids (lattices) of arbitrary size $N \times M \times L$. The LBM module uses 3×3 (D2Q9), 19 (D3Q19), and $3 \times 3 \times 3$ (D3Q27) velocity lattices. The FV LBM implementation in UFS follows that of Ref. [31]. Special mapping procedures and structures map UFS's regular Cartesian velocity grid to the LBM velocity grids. These structures also contain the weights of each LBM velocity vector required to compute the equilibrium distribution function for initial and boundary conditions and for the BGK-LBM collisional integral.

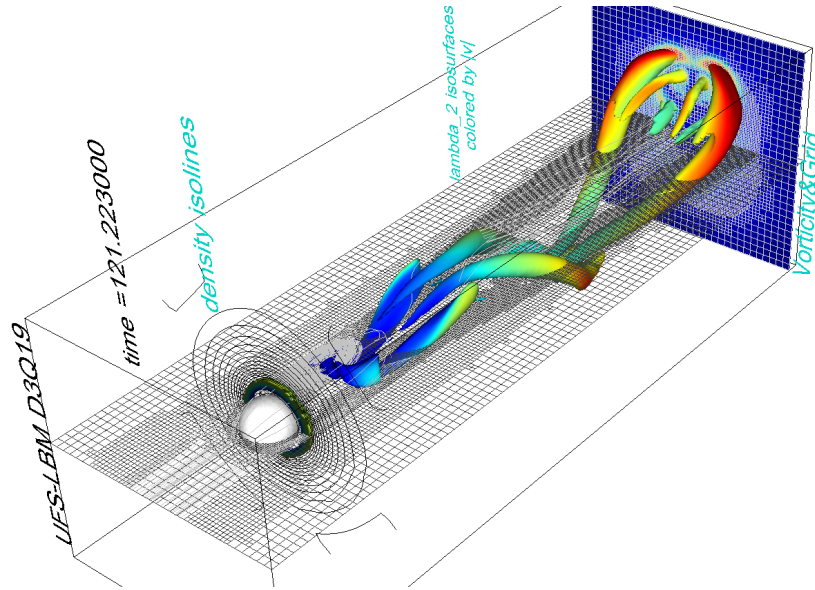


Figure 9: Complex 3D structure of the periodic wake obtained with UFS-LBM D3Q19 model. The vertical cross-section is colored according to the vorticity. The horizontal and vertical cross-sections display the depth of refinement of the adaptive mesh.

The SFC algorithm is used for parallelization of the LBM module. Figure 9 shows an example of parallel simulations on 8 PEs of gas flow over a sphere at Mach=0.5 and Re=1,000 with D3Q19 model. The obtained complex structure of the periodic wake is illustrated by iso-surfaces of the (eigenvalue) lambda2 criterion of Jeong and Hussain at two different time instances. One can see that computational grid adapts well to the flow vorticity, and the DLB algorithm keeps the numbers of cells per PE close even when the number of cells increases more than 10 fold during the run . The lambda2 criterion allows uniquely visualizing the formation of hairpin vortices in 3D geometry. Comparison with other codes showed the validity of our UFS-LBM implementation with adaptive Cartesian mesh. As expected an ideal DLB was observed with the SFC algorithm.

GPU accelerated LBM Solver

GPU acceleration of the transport module in LBM is the most crucial because the collisional (LBM-BGK) module takes only 20% of the total computational cost. The main idea behind the new LBM-tuned kernels relied on the fact that the number of velocity grid points is small in LBM and the number of spatial cells can be very large. This allows us to group each velocity grid in a spatial cell into a warp. The concept of thread groups or warps is fundamental to the GPU's operation; warps are groups of threads handled in parallel by the GPU's execution units. For a D3Q27 model, the number of velocity grid points is 27 and the warp size is 32. This means that almost the whole warp will be processing the velocity grid points in parallel (with only 5 threads remaining idle). We then group 16 or 32 warps into a block and the number of blocks is decided upon the total number of spatial cells. Since the transport module in UFS-LBM involves summations over neighboring cells (which can be any number from 6 to 6×4 on an Octree mesh depending on the level of refinement of each particular spatial cell), a warp which finishes computations first will switch to another warp and so on. As pointed out in Ref. [32], when one

warp stalls on a memory operation, the multiprocessor selects another ready warp and switches to that one; in this way, the cores can be productive as long as there is enough parallelism to keep them busy. This allows the computations to proceed without delay on a large number of cells of different neighbor topologies, which is particularly important for an octree mesh.

GPU speedup has been tested for the same 3D flow past a sphere presented above. We have verified that the obtained CPU and GPU results coincide within a machine precision. We compared times required to execute one transport and one collisional step on CPU and on GPU for two types of grids with $\sim 100K$ and $\sim 1M$ cells. Table 1 shows results for two GPU cards (Fermi and Kepler) (results are for kernel-only computations discarding pre- and post-processing times). One can see that the advection kernel shows speedup factors ~ 40 for the Tesla C2070 and ~ 60 for the Tesla K20c card. As expected, the speedup factors are larger for the Tesla K20c because it is a more powerful GPU. The collisional kernel achieves even larger speedup factors of ~ 150 for both cards. However, the collisional kernel takes a small fraction of the total advection-collision step, and the overall contribution of the collisional kernel speed up is small. We have observed that the speedup factors of the advection and collision kernels are the same for both grids of different size. This is an indication that the kernels are properly implemented and no degradation of performance is observed for grids of different size. This fact is particularly important for dynamically adapting grids with the cell count changing by up to 2 orders of magnitude during a simulation.

TABLE 1. UFS-LBM GPU speedup observed on Tesla C2070 and K20c cards.

GPU Card	C2070	K20c	C2070	K20c
Spatial grid size (cells)	100K	100K	1M	1M
Advection speedup	36	59	37	58
Collision speedup	150	151	158	155
Ratio Advection/Collision	2.3	2.4	2.3	2.4

CONCLUSIONS

We have described multi-GPU implementation of three kinetic modules in UFS: the DVM Boltzmann solver, the DSMC module, and the LBM solver. This implementation has taken advantages of the octree, dynamically adaptive grids with capabilities to automatically mesh solid objects of complex shape, moving-body capabilities, Space-Filling-Curve (SFC) and Forrest-of-Trees (FOT) MPI parallel capabilities with efficient Dynamic Load Balancing (DLB). The DVM Boltzmann solver was parallelized using the SFC algorithm, the DSMC module was parallelized using the FOT algorithm. Double digit speedup on single GPU and good scaling for multi-GPU have been demonstrated.

We have developed a new LBM-based mesoscopic solver and demonstrated efficient AMR and multi-CPU capabilities of the solver. We have successfully implemented new GPU kernels for the advection (transport) and collisional modules taking into account peculiarities of the LBM code on (semi-structured) spacetime meshes (warp-based data treatment). We have observed speedups of $\sim 60x$ for the advection GPU kernel and $\sim 150x$ for the collisional kernel. The implementation demonstrated good scalability on grids of different size. Further work will focus on resolving contradicting requirements of AMR and GPU, and combine advantages of octree-type meshes with regularly refined patches (blocks) desirable for GPU computing.

ACKNOWLEDGMENTS

The work of Sergey Zabelok was supported by the Program No. 15 of the Presidium of Russian Academy of Sciences. The work at CFDRC was partially supported by the DoE SBIR Phase I Project DE-SC0010148. We wish to thank Martin Burtcher for useful discussions and suggestion of the warp algorithm for the LBM solver.

REFERENCES

-
- ¹ V.I.Kolobov, R.R. Arslanbekov, V.V.Aristov, A.A.Frolova, S.A.Zabelok, Unified solver for rarefied and continuum flows with adaptive mesh and algorithm refinement, *J. Comput. Phys.* **223** (2007) 589.
 - ² V.I.Kolobov and R.R.Arslanbekov, Towards Adaptive Kinetic-Fluid Simulations of Weakly Ionized Plasmas, *J. Comput. Phys.* 231 (2012) 839
 - ³ M Rieke, T Trost, R.Grauer, Coupled Vlasov and two-fluid codes on GPUs, *J. Comput. Phys.* 283 (2015) 436
 - ⁴ C K Birdsall, A B Langdon, *Plasma Physics via Computer Simulations*, Taylor and Francis (2004).
 - ⁵ G.A. Bird, *Molecular Gas Dynamics and the Direct Simulation of Gas Flows*, Oxford Science Publications (1994).
 - ⁶ V.V.Aristov, *Direct Methods for Solving the Boltzmann Equation and Study of Non-Equilibrium Flows*, Kluwer Academic Publishers, Dordrecht (2001).
 - ⁷ M. Shoucri (Editor), *Eulerian Codes for the Numerical Solution of the Kinetic Equations of Plasmas*, Nova Publishers (2010).
 - ⁸ A.L. Garsia, J.B. Bell, W.Y. Crutchfield and B.J. Alder, Adaptive Mesh and Algorithm Refinement using Direct Simulation Monte Carlo, *J. Comp. Phys.* **54** (1999) 134.
 - ⁹ R.R. Arslanbekov, V.I. Kolobov, and A.A. Frolova, Analysis of Compressible Viscous Flow Solvers with Adaptive Cartesian Mesh, 20th AIAA Computational Fluid Dynamics Conference, 2011, AIAA 2011-3381.
 - ¹⁰ R. Mehta, V.I. Kolobov, R.R. Arslanbekov, A. Feldick, M. Modest, Hybrid Radiation Transport Model for Weakly Ionized Plasma, AIAA-2011-3767.
 - ¹¹ Gerris Flow Solver: http://gfs.sourceforge.net/wiki/index.php/Main_Page
 - ¹² G. Agbaglah, et al, "Parallel simulation of multiphase flows using octree adaptivity and the volume-of-fluid method," *Comptes Rendus Mécanique* 339 (2011) 194.
 - ¹³ R.R.Arslanbekov, V.I.Kolobov, and A.A.Frolova, Kinetic Solvers with Adaptive Mesh in Phase Space, *Phys. Rev. E* **88** (2013) 063301.

-
- ¹⁴ R.R. Arslanbekov, V.I. Kolobov, J. Burt, E. Josyula, Direct Simulation Monte Carlo with Octree Cartesian Mesh, AIAA 2012-2990
- ¹⁵ S Zabelok, R Arslanbekov, V Kolobov, “Multi-GPU kinetic solvers using MPI and CUDA”, Rarefied Gas Dynamics. Proc. 29th Int. Symp., AIP Conference Proceedings 1628, ed. Jing Fan, Melville, New York, 2014, p. 539-546
- ¹⁶ <http://gpuscience.com>
- ¹⁷ C.A.Navarro, N Hitschfeld-Kahler, L.Mateu, A survey on parallel computing and its applications in data-parallel problems using GPU architectures, Commun. Comput. Phys. **15** (2014) 285.
- ¹⁸ <http://iss.ices.utexas.edu/?p=projects/galois/lonestargpu>
- ¹⁹ M.J. Goldsworthy, A GPU–CUDA based direct simulation Monte Carlo algorithm for real gas flows, Computers & Fluids 94 (2014) 58–68
- ²⁰ A Kashkovsky, 3D DSMC computations on a heterogeneous CPU-GPU cluster with a large number of GPUs, AIP Conference Proceedings 1628, 192 (2014)
21. Y. Kloss, P. Shuvalov, and F. Tcheremissine, Solving Boltzmann equation on GPU, Procedia Computer Science **1**, 1083-1091 (2010).
22. A. Frezzotti, G. Ghioldi, and L. Gibelli, Solving the Boltzmann equation on GPUs, Computers & Fluids **50**, 136-146 (2011).
23. S.A. Zabelok, R.R. Arslanbekov, V.I. Kolobov, GPU Accelerated Kinetic Solvers for Rarefied Gas Dynamics AIAA Paper 2013-2863.
- ²⁴ S.A. Zabelok, V.V. Aristov, A.A. Frolova, V.I. Kolobov and R.R. Arslanbekov, “Parallel implementation of the Unified Flow Solver”, Rarefied Gas Dynamics: 25 International Symposium, St. Petersburg, Russia (2006).
- ²⁵ S.A. Zabelok, R.R. Arslanbekov, V.I. Kolobov, GPU Accelerated Kinetic Solvers for Rarefied Gas Dynamics, AIAA Paper 2013-2863.
- ²⁶ E. A. Malkov, M. S. Ivanov, S. O. Poleshkin, “Discrete velocity scheme for solving the Boltzmann equation accelerated with the GP GPU”, in *28th International Symposium on Rarefied Gas Dynamics 2012*, edited by M. Mareshal and A. Santos, AIP Conference Proceedings 1501, American Institute of Physics, Melville, NY, 2012, pp. 318-325.
- ²⁷ S. A. Zabelok, A. V. Stroganov, V. V. Aristov, “Deterministic GPU Boltzmann solver”, in Rarefied Gas Dynamics. Proc. 29th Int. Symp., AIP Conference Proceedings 1628, ed. Jing Fan, Melville, New York, 2014, p. 1009-1015

²⁸ R.R.Arslanbekov, V.I.Kolobov, and A.A.Frolova, "Immersed Boundary Method for Boltzmann and Navier-Sokes Solvers with Adaptive Cartesian Mesh", 27 Symposium on Rarefied Gas Dynamics, 2010, AIP Conf. Proc. 1333 (2011) 873.

²⁹ GNU Triangulated Surface Library, <http://gts.sourceforge.net/>

³⁰ Su C.-C., Smith M. R., Kuo F.-A., Wua J.-S., Hsieh C.-W., and Tseng K.-C., "Large-Scale Simulations on Multiple Graphics Processing Units (GPUs) for the Direct Simulation Monte Carlo Method," J. Comp. Phys. 231 (2012) 7932.

³¹ . D. V. Patil and K. N. Lakshmisha, "Finite Volume TVD Formulation of Lattice Boltzmann Simulation on Unstructured Mesh", J. Comput. Phys. **228**, 5262-5279 (2009).

³² . M. Wolfe, Understanding the CUDA Data Parallel Threading Model, <https://www.pgroup.com/lit/articles/insider/v2n1a5.htm>